
TISSUE CONCEPTS v2: A SUPERVISED FOUNDATION MODEL FOR WHOLE SLIDE IMAGES

Till Nicke
Fraunhofer MEVIS
Lübeck, Germany
till.nicke@mevis.fraunhofer.de

Daniela Scharcherer
Fraunhofer MEVIS
Bremen, Germany

Jan Raphael Schäfer
Fraunhofer MEVIS
Bremen, Germany

Natalia Artysh
Fraunhofer ITEM
Hannover, Germany;
Department of Pulmonology
Hannover Medical School, Hannover, Germany

Antje Prasse
Fraunhofer ITEM
Hannover, Germany;
Department of Pulmonology
Hannover Medical School, Hannover, Germany;
Prasse Lab, Department of Biomedicine,
University of Basel, Basel, Switzerland

André Homeyer
Fraunhofer MEVIS
Bremen, Germany

Andrea Schenk
Fraunhofer MEVIS
Bremen, Germany;
Institute for Diagnostic and Interventional Radiology
Hannover Medical School, Hannover, Germany

Henning Höfener *
Fraunhofer MEVIS
Bremen, Germany

Johannes Lotz *
Fraunhofer MEVIS
Lübeck, Germany

ABSTRACT

Foundation models (FMs) are transforming the field of computational pathology by offering new approaches to analyzing histopathology images. Typically relying on weeks of training on large databases, the creation of FMs is a resource-intensive process in many ways. In this paper, we introduce the extension of our supervised foundation model, Tissue Concepts, to whole slide images, called Tissue Concepts v2 (TCv2), a supervised foundation model for whole slide images to address the issue above. TCv2 uses supervised, end-to-end multitask learning on slide-level labels. Training TCv2 uses a fraction of the training resources compared to self-supervised training. The presented model shows superior performance compared to SSL-trained models in cancer subtyping benchmarks and is fully trained on freely available data. Furthermore, a shared trained attention module provides an additional layer of explainability across different tasks.

Keywords end-to-end learning · multiple-instance learning · Foundation Model · Tissue Concepts

*Henning Höfener and Johannes Lotz contributed equally.

1 Introduction

Foundation models (FMs) are transforming the field of computational pathology by offering a new approach to analyzing digital histopathology images. Traditionally, diagnosing whole-slide images (WSIs) is a labor-intensive process for pathologists, often limited by inter-observer variability and the sheer volume of data. FMs have shown the ability to generalize across various tasks and their broad applicability promises to significantly reduce the workload of pathologists, enabling more efficient and accurate diagnosis and research.

Most FMs operate at the patch level, creating generic feature vectors from small patch images of a few hundred pixels side length that can be used for various decision-making purposes. More recent advances target slide-level embeddings, whereby one WSI can be represented by a single embedding vector. To achieve this, a two-step training process is widely adopted. In various studies, a pre-trained, frozen patch encoder is used to extract patch-level features, which are then further processed, mostly using self-supervised learning (SSL), to encode slide-level embeddings [1, 2, 3, 4].

Since the patch encoder is not usually adapted for slide-level embedding, the patch features may not necessarily be optimal for slide-level tasks. Furthermore, self-supervised training of two separate model components requires substantial computing power and a large amount of data [5]. Moreover, most of the models presented in current studies rely heavily on closed-source data, which limits the reproducibility and bias exploration of these methods, even when weights and code are released.

Recently, we showed that multi-task learning is an energy- and data-efficient way of training foundation models [5]. The FM Tissue Concepts were trained using patch-based level labels, such as patch classification, segmentation, and detection. This paper extends the pipeline and introduces Tissue Concepts v2 (TCv2), a new supervised foundation model for whole slide images that addresses the aforementioned issues as follows:

- End-to-end multitask learning [6] on slide-level labels makes the model more resource-efficient than self-supervised training while exhibiting state-of-the-art performance in various tasks.
- Through supervised learning, slide-level features important for overall survival or genetic mutations are directly encoded into the model.
- Using only openly available data, primarily from the National Cancer Institute (NCI) Imaging Data Commons (IDC) [7], the presented methods are easily reproducible.

2 Related Work

The uni-modal Prov-GigaPath [3] model is based on a ViT patch encoder followed by an aggregation network. The patch encoder was trained using self-supervision on a private dataset. On top of the patch encoder, a slide-level encoder was trained using masked tile modeling, a latent version of masked image modeling, on the same dataset. The slide encoder is based on LongNet [8] with dilated attention to incorporate more patches into the sequence.

A uni-modal approach was also applied by Lenz et al. [2], who used different patch encoders to train a slide-level encoder based on contrastive learning. The same patches from a WSI were passed through different patch encoders to create different views of the same images. The slide encoder was then trained with contrastive loss to increase the similarity between the pooled versions of the encoded patches.

A different, multi-modal approach was presented by Wang and colleagues [9]. CHIEF is based on the CTransPath patch encoder combined with a CLIP text embedding. The anatomical sites of the WSIs were transformed into the text embedding and added to the aggregated latent vector of the patches transformed by CTransPath.

TITAN [1] was also trained on multi-modal data by first training a slide-level encoder based on student-teacher learning and then aligning the encoded slides with either generated captions or real-world pathology reports.

PRISM [4] presents a similar approach, where a slide encoder was trained in combination with a BioGPT language model to align slide-level features with the corresponding language embeddings.

While these methods exhibit strong performance, they rely on multi-step approaches, where first, a patch extractor or text embedding needs to be trained, typically using SSL, and second, an aggregation method is applied to the extracted embeddings. However, supervised end-to-end learning is a valuable strategy for solving multi-instance learning problems for slide-level labels [10, 11].

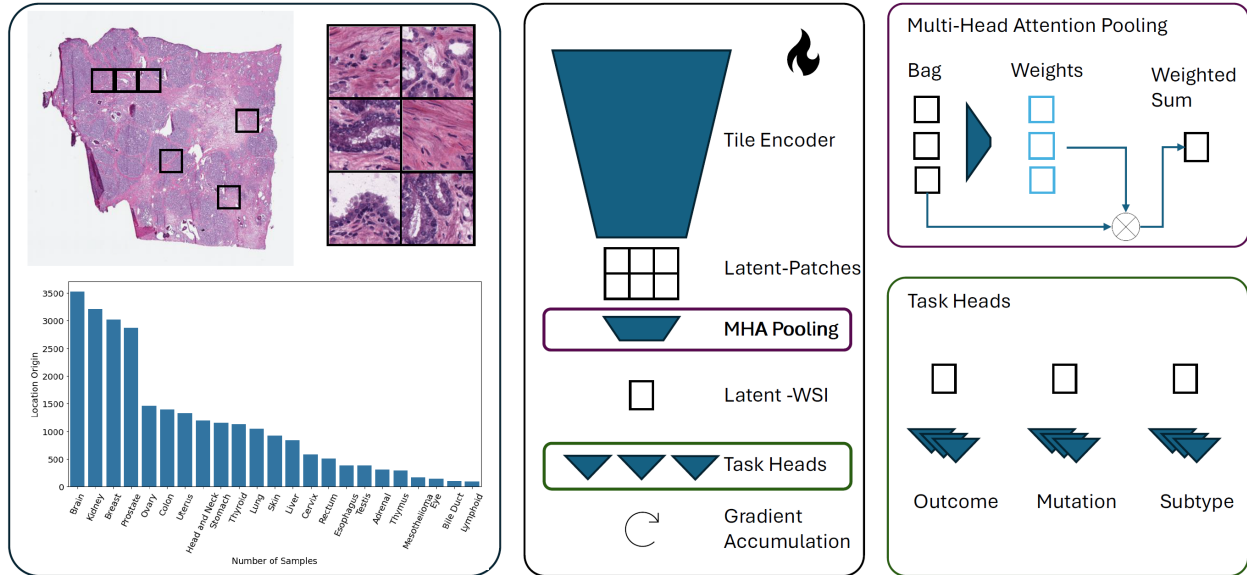


Figure 1: Schematic overview of the pipeline. A collection of WSI with corresponding labels (left) is used to train a tile encoder and pooling operation using multi-task learning (middle). The training is done in an end-to-end manner, iterating over individual tasks (lower right) and accumulating the gradient. Learnable weights rate each instance of the bag and then compress it into a latent WSI vector (top right).

3 Methods

We propose a supervised, multi-task training scheme that is purely based on whole-slide-level labels from the TCGA, CPTAC, and PLCO datasets. Figure 1 provides a schematic overview of the training strategy. Within-bag sampling allows for efficient end-to-end training of the tile encoder and the slide-level multi-head attention (MHA) pooling. Latent patches are rated with respect to their significance and then pooled by a weighted sum into a single latent WSI representation (Figure 1 top right). Since the pooling operation is shared between all individual tasks, a general WSI representation space is learned such that all tasks can be solved individually from it.

3.1 Training data

To train the foundation model, data from the TCGA, CPTAC, and PLCO cohorts were collected. All data is openly accessible, which enables reproducing our results and model. It also enables research towards biases within our model based on the input images.

TCGA and CPTAC data were obtained from the IDC. The IDC is a cloud-based repository of public cancer data, hosting images and analysis results from different modalities including brightfield and fluorescence slide microscopy. All data in the IDC are harmonized into the Digital Imaging and Communications in Medicine (DICOM) format, versioned, and searchable by DICOM and non-DICOM metadata to facilitate transparency and reproducibility in imaging research studies [12, 13, 14]. We share the search query to obtain the TCGA and CPTAC data used in this study in the appendix queries 1, 2. Training data was obtained mainly from the TCGA data cohort, while the CPTAC cohort was held out for testing.

The PLCO cohort consists of 881 cases of radical prostatectomy (184 with event) with 2999 H&E stained WSIs. The cohort was cleaned to contain only cases with usable endpoints, leaving 875 (182) cases with 2352 slides. The cohort was then split (80/20) into a train and validation subset. Unfortunately, the PLCO cohort is not as easily accessible as the TCGA or CPTAC cohorts but requires a written request.

From the TCGA and PLCO cohorts, we created 18 different tasks, listed in Table 2, all of which had one label per slide. Subtyping targets were created through the TCGA-internal information such as the diagnosed BRCA subtypes, or diagnosed ISUP scores for prostate cancer. Survival and mutation targets were extracted from cBioPortal [15]. We ensured that training and validation splits were coherent across tasks. For example, TCGA-NSCLC comprises the TCGA-LUAD and TCGA-LUSC cohorts, which share some slides with the task for TCGA-LUSC-TP53 prediction. For both tasks, we ensured that the same validation slides were not included in the training set of the other task.

3.2 Multi-task, end-to-end training pipeline

The pipeline shown in Figure 1 (center) was trained using multi-task learning, where each task, presented in Table 2, was solved by a separate, small linear head. The head consisted of a 10% dropout layer followed by the decision layer. Each training bag consisted of 64 to 128 randomly selected patches from a single WSI. All instances of one bag were passed through a shared encoder and pooled by a multi-head attention module [16], consisting of 8 heads, which weighted each instance of the bag and compressed the bag into one feature vector. This WSI vector was then used as input to a classification head based on the respective task. By iterating through the tasks and accumulating each loss, a combined optimizer step could be performed, solving all tasks simultaneously [6]. As a backbone, a tiny Swin-transformer V2 [17] was used and initialized with Tissue Concepts weights [5]. During training, each patch in each bag was individually augmented using standard augmentation such as color shift, blurring, gray scaling, and deforming. Validation bags were not augmented and always contained 128 patches, the maximum size of a training bag. The pipeline was trained for 200 epochs while monitoring the validation loss and the best validation model was selected for testing. The entire pipeline was trained on one NVIDIA A100 for approximately 500 hours.

3.3 Evaluation

For evaluation, we selected smaller cohorts based on challenges or openly available datasets. We created separate in- and out-of-domain evaluation tasks to fully assess the performance of the TCv2 model.

The BReAst Cancer Subtyping (BRACS) dataset consists of 547 WSIs from 189 patients which are already divided into training (395), validation (87) and test (65) splits [18]. The WSIs can be divided into three target classes: Benign, Atypical, and Malignant. The balanced accuracy and area under the ROC curve (AUC) were used as test metrics.

The lung fibrosis estimation task is based on an internal dataset obtained at the Fraunhofer ITEM in Hannover. It includes 94 H&E-stained precision-cut lung slices (PCLS) and corresponding tri-chrome-stained slides (split into 45/20/29 for training, validation, and testing) obtained and scanned at 20x from 10 donors. The tri-chrome-stained images were segmented using the semi-automatic software HistoKat [19, 20]. The area percentage of collagen, lung parenchyma, other tissue, and background was computed on the segmentation masks. The same overall collagen distribution was assumed for the corresponding H&E stained slide pair, generating slide-level labels for each H&E stained slide. The dataset’s median segmented collagen area proportion was defined as a threshold for low or high collagen classes. We measured the AUC and balanced accuracy as evaluation metrics.

The CPTAC-NSCLC subset is used as an in-domain evaluation task (with TCGA-NSCLC used during pre-training). It contains slides from 432 patients and was divided into train, validation, and test (40/10/50) splits. The task was to distinguish between lung adenocarcinoma and lung squamous cell carcinoma. Balanced accuracy and AUC were used as evaluation metrics.

The Prostate cANcer graDe Assessment (PANDA) challenge provides 10616 openly available WSIs from two different centers, Karolinska and Radboud [21]. A consensus ISUP score is assigned to each WSI. The score ranges from 0 (normal tissue) to 5 (severe prostate cancer). The evaluation task was to predict the ISUP score from the images. The dataset was split into train validation and testing (50/10/40), with a focus on balanced ISUP representations in each set. AUC and Cohen’s quadratic kappa were used as evaluation metrics.

4 Results

4.1 Performance

We compare the results of Tissue Concepts v2 with the previously presented Tissue Concepts [5] encoder. Both share the same backbone architecture. The ABMIL module was initialized with random weights for the TC encoder and with the pre-trained weights for TCv2. For all validation tasks, the encoder weights were frozen and only the aggregation module was fine-tuned. AdamW with a learning rate of 10^{-4} was used for 15 epochs while monitoring the validation loss to select the best-performing model for testing. Fine-tuning and testing were repeated 4 times to account for randomization effects. The average metrics for the corresponding test sets are reported in Table 1.

In the in-domain task, CPTAC-NSCLC, the TCv2 model reached a higher average AUC (0.95) compared to the TC patch encoder (0.87). Additionally, the TCv2 outperforms the reported performance measurements for the CHIEF model [9], despite both models sharing the same backbone architecture. Notably, CHIEF was additionally trained on multi-domain data. TCv2 also outperforms Prov-GigaPath [3] on this task, even though Prov-GigaPath is reported to have a much larger parameter count (ca. 28M versus ca. 1.1B [22]).

Table 1: Area under the ROC curve (AUC), balanced accuracy (b ACC), and Cohen’s quadratic kappa were evaluated on 4 evaluation tasks. On each task, Tissue Concepts v2 (TCv2, presented here) was compared with the patch-based Tissue Concepts (TC) and other self-supervised foundation models if matching experiments were available in the literature.

Test Task	Model	AUC	b ACC	Cohen’s kappa
CPTAC-NSCLC	TC	0.87 ± 0.06	0.84 ± 0.10	-
	CHIEF [9]	0.91 ± 0.01	-	-
	Prov-GigaPath [3]	0.80 ± 0.01	0.61 ± 0.01	-
	TCv2	0.95 ± 0.01	0.905 ± 0.05	-
PANDA	TC	0.52 ± 0.06	-	0 ± 0
	TCv2	0.84 ± 0.02	-	0.68 ± 0.05
BRACS	TC	0.70 ± 0.07	0.40 ± 0.08	-
	CHIEF [1]	-	0.63 ± 0.05	-
	Prov-GigaPath [1]	-	0.56 ± 0.1	-
	TCv2	0.84 ± 0.01	0.63 ± 0.02	-
Fibrosis	TC	0.84 ± 0.02	0.72 ± 0.11	-
	TCv2	0.86 ± 0.02	0.73 ± 0.07	-

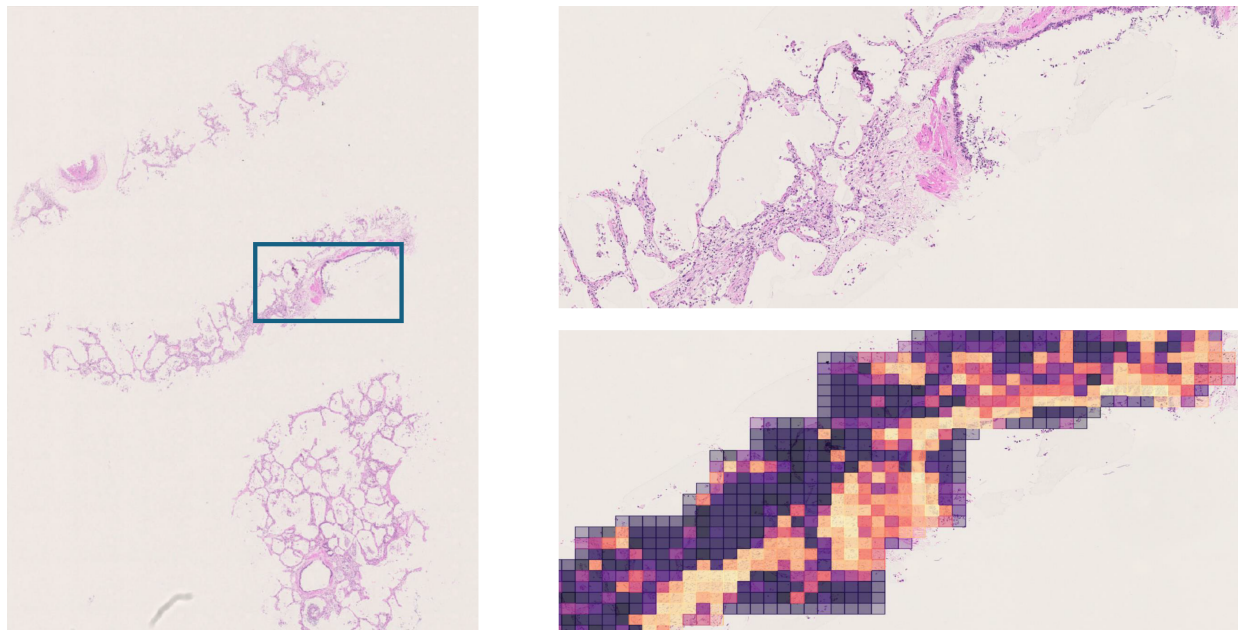


Figure 2: Attention weight visualization of a model fine-tuned for lung fibrosis estimation.

In the other in-domain task PANDA, TCv2 achieves a higher average AUC (0.84) compared to the TC model with a randomly initialized aggregation module (0.52). The patch-based encoder was unable to solve the task, as indicated by the test Cohen’s kappa score of 0.0.

In the out-of-domain BRACS task, TCv2 also outperforms the previous TC encoder, achieving an AUC of 0.84 compared to 0.70. In [1], Ding et al. compare Prov-GigaPath and CHIEF on this task as well and report the balanced accuracies. TCv2 outperforms Prov-GigaPath on this metric and performs on par with CHIEF. Similarly, in the out-of-domain fibrosis estimation task, TCv2 outperforms the patch-based foundation model TC by 2 percentage points (0.86 versus 0.84).

4.2 Explainability

Through the attention pooling module, the relative patch importance for each task can be computed, providing a layer of explainability. We fine-tuned the model to estimate the collagen area fraction and visualized the attention weights in Figure 2. The network effectively highlights areas of high collagen in H&E stained images of PCLS.

5 Discussion

In this paper, we show that end-to-end learning using weakly supervised labels is an efficient approach to creating whole slide image foundation models.

The training of TCv2 demonstrates that self-supervised training while creating robust and capable models, is less efficient for creating vision foundation models in digital pathology. Comparing TCv2 on the in-domain NSCLC benchmark against CHIEF[9] and Prov-GigaPaths[3], TCv2 outperforms both models. In the out-of-domain BRACS evaluation, TCv2 outperforms Prov-GigaPath and achieves comparable results to the CHIEF model according to the evaluation performed by Ding et al.[1].

A limitation of the current evaluation is that testing on only four different tasks may not be sufficient to fully assess the presented model. Additionally, the feature extractor is based on a tiny Swin-transformer. A comparison and scaling to a larger Swin-transformer is still missing and could lead to improved performance. Previous results show that patch-based multi-task learning yields robust results with fewer training images compared to patch-based SSL. A combination of weakly-labeled WSIs and patch-based tasks is the next logical step.

Considering the high amount of energy needed to train not only large language models but also vision foundation models in digital pathology, weakly supervised end-to-end learning using MTL appears to be substantially more energy efficient compared to SSL-based methods. Considering the training time of 500 hours of the presented pipeline, and assuming that the GPU was working under full load for the whole time (400 W), the training used around 200kWh of electric energy overall. Since the model was trained on a cluster located in Germany, this amounts to 70 to 105 kg of CO_2 emitted by the training process ($0.35kgCO_2/kWh^{2.3}$). Additionally, since the training started from the Tissue-Concepts checkpoint [5], another 20 kg of CO_2 have to be taken into account from the previous training of 160 RTX A5000 hours. This results in a total emission of 90-125 kg of CO_2 . Compared to other models, TCv2's training footprint is very small. In [3] the authors report a training time of 3072 A100 hours for the slide encoder of the Prov-GigaPath model. This amounts to approximately 500 kg of CO_2 emissions for this single component. The training time of the tile encoder, which likely exceeds the training of the slide encoder, was not mentioned. In comparison, the complete training of TCv2 used between 18 and 25% of the emissions of the slide encoder of Prov-GigaPath alone. CTransPath [23], the backbone of CHIEF [9] trained for a reported 12000 hours on an NVIDIA V100 GPU. TCv2 overall used 660 hours of computing or 5% of the time needed to train a single patch encoder. A similar comparison has been made by Campanella et al. [22], who compared the training time in hours on multiple A100 or V100 80GB GPUs. They report that UNI [24] trained for about 1000 hours on an A100 GPU, which is double the training time needed to create the tile encoder.

Relying on openly available data facilitates reproducibility, even when the weights of the model are also open-sourced. In addition, other researchers can more easily investigate and counteract known or unknown biases inherent in the training data. This can, in turn, lead to community-driven improvements in the models themselves. Versioning of files in the IDC allows researchers to address issues like misclassifications of single files. For future reproducibility studies, the same files can be accessed. In the case of the PLCO prostate data, a short application is required.

6 Conclusion

In this paper, we demonstrate that MTL is an efficient approach to train a supervised foundation model from weakly supervised labels. The presented model, Tissue Concepts v2, shows improved performance over the first version of the MTL-trained tile encoder ("Tissue Concepts") and other foundation models on several benchmarks. By using slide-level labels in combination with 18 different tasks, the model could be trained in an end-to-end manner, showing reduced energy and data requirements over self-supervised trained models. TCv2 exhibits a ca. 20% power usage over other models during training. Additionally, the model was trained on freely available data, enhancing reproducibility.

7 Acknowledgements

This work was partially funded by the Fraunhofer-Gesellschaft through the Project FibroPaths.

The results published here are in part based on data generated by the TCGA Research Network: <https://www.cancer.gov/tcga>.

²<https://www.umweltbundesamt.de/themen/co2-emissionen-pro-kilowattstunde-strom-2024>

³<https://ourworldindata.org/grapher/carbon-intensity-electricity>

Data used in this publication were generated in part by the National Cancer Institute Clinical Proteomic Tumor Analysis Consortium (CPTAC).

The authors thank the National Cancer Institute for access to NCI’s data collected by the Prostate, Lung, Colorectal, and Ovarian (PLCO) Cancer Screening Trial (CDAS PROJECT NUMBER: PLCOI-1612).

References

- [1] Tong Ding, Sophia J Wagner, Andrew H Song, Richard J Chen, Ming Y Lu, Andrew Zhang, Anurag J Vaidya, Guillaume Jaume, Muhammad Shaban, Ahrong Kim, et al. Multimodal whole slide foundation model for pathology. *arXiv preprint arXiv:2411.19666*, 2024.
- [2] Tim Lenz, Peter Neidlinger, Marta Ligeró, Georg Wölflein, Marko van Treeck, and Jakob Nikolas Kather. Unsupervised foundation model-agnostic slide-level representation learning. *arXiv preprint arXiv:2411.13623*, 2024.
- [3] Hanwen Xu, Naoto Usuyama, Jaspreet Bagga, Sheng Zhang, Rajesh Rao, Tristan Naumann, Cliff Wong, Zelalem Gero, Javier González, Yu Gu, et al. A whole-slide foundation model for digital pathology from real-world data. *Nature*, 630(8015):181–188, 2024.
- [4] George Shaikovski, Adam Casson, Kristen Severson, Eric Zimmermann, Yi Kan Wang, Jeremy D Kunz, Juan A Retamero, Gerard Oakley, David Klimstra, Christopher Kanan, et al. Prism: A multi-modal generative foundation model for slide-level histopathology. *arXiv preprint arXiv:2405.10254*, 2024.
- [5] Till Nicke, Jan Raphael Schäfer, Henning Höfener, Friedrich Feuerhake, Dorit Merhof, Fabian Kießling, and Johannes Lotz. Tissue concepts: Supervised foundation models in computational pathology. *Computers in Biology and Medicine*, 186:109621, 2025.
- [6] Raphael Schäfer, Till Nicke, Henning Höfener, Annkristin Lange, Dorit Merhof, Friedrich Feuerhake, Volkmar Schulz, Johannes Lotz, and Fabian Kiessling. Overcoming data scarcity in biomedical imaging with a foundational multi-task model. *Nature Computational Science*, 4(7):495–509, 2024.
- [7] Andrey Fedorov, William JR Longabaugh, David Pot, David A Clunie, Steve Pieper, Hugo JWL Aerts, André Homeyer, Rob Lewis, Afshin Akbarzadeh, Dennis Bontempi, et al. Nci imaging data commons. *Cancer research*, 81(16):4188–4193, 2021.
- [8] Jiayu Ding, Shuming Ma, Li Dong, Xingxing Zhang, Shaohan Huang, Wenhui Wang, Nanning Zheng, and Furu Wei. Longnet: Scaling transformers to 1,000,000,000 tokens. *arXiv preprint arXiv:2307.02486*, 2023.
- [9] Xiyue Wang, Junhan Zhao, Eliana Marostica, Wei Yuan, Jietian Jin, Jiayu Zhang, Ruijiang Li, Hongping Tang, Kanran Wang, Yu Li, et al. A pathology foundation model for cancer diagnosis and prognosis prediction. *Nature*, 634(8035):970–978, 2024.
- [10] Shuai Jiang, Arief A Suriawinata, and Saeed Hassanpour. Mhattsurv: Multi-head attention for survival prediction using whole-slide pathology images. *Computers in biology and medicine*, 158:106883, 2023.
- [11] Jiangping Wen, Jinyu Wen, and Meie Fang. Msamil-net: An end-to-end multi-scale aware multiple instance learning network for efficient whole slide image classification. *arXiv preprint arXiv:2503.08581*, 2025.
- [12] Andrey Fedorov, William JR Longabaugh, David Pot, David A Clunie, Steven D Pieper, David L Gibbs, Christopher Bridge, Markus D Herrmann, André Homeyer, Rob Lewis, et al. National cancer institute imaging data commons: toward transparency, reproducibility, and scalability in imaging artificial intelligence. *Radiographics*, 43(12):e230180, 2023.
- [13] Daniela P Schacherer, Markus D Herrmann, David A Clunie, Henning Höfener, William Clifford, William JR Longabaugh, Steve Pieper, Ron Kikinis, Andrey Fedorov, and André Homeyer. The nci imaging data commons as a platform for reproducible research in computational pathology. *Computer methods and programs in biomedicine*, 242:107839, 2023.
- [14] Dennis Bontempi, Leonard Nuernberg, Suraj Pai, Deepa Krishnaswamy, Vamsi Thiriveedhi, Ahmed Hosny, Raymond H Mak, Keyvan Farahani, Ron Kikinis, Andrey Fedorov, et al. End-to-end reproducible ai pipelines in radiology using the cloud. *Nature Communications*, 15(1):6931, 2024.
- [15] Ethan Cerami, Jianjiong Gao, Ugur Dogrusoz, Benjamin E Gross, Selcuk Onur Sumer, Bülent Arman Aksoy, Anders Jacobsen, Caitlin J Byrne, Michael L Heuer, Erik Larsson, et al. The cbio cancer genomics portal: an open platform for exploring multidimensional cancer genomics data. *Cancer discovery*, 2(5):401–404, 2012.
- [16] Maximilian Ilse, Jakub Tomczak, and Max Welling. Attention-based deep multiple instance learning. In *International conference on machine learning*, pages 2127–2136. PMLR, 2018.

- [17] Ze Liu, Han Hu, Yutong Lin, Zhuliang Yao, Zhenda Xie, Yixuan Wei, Jia Ning, Yue Cao, Zheng Zhang, Li Dong, et al. Swin transformer v2: Scaling up capacity and resolution. In *Proceedings of the IEEE/CVF conference on computer vision and pattern recognition*, pages 12009–12019, 2022.
- [18] Nadia Brancati, Anna Maria Anniciello, Pushpak Pati, Daniel Riccio, Giosuè Scognamiglio, Guillaume Jaume, Giuseppe De Pietro, Maurizio Di Bonito, Antonio Foncubierta, Gerardo Botti, et al. Bracs: A dataset for breast carcinoma subtyping in h&e histology images. *Database*, 2022:baac093, 2022.
- [19] Henning Höfener. *Automated Quantification of Cellular Structures in Histological Images*. PhD thesis, Universität Bremen, 2019.
- [20] Janine Arlt, André Homeyer, Constanze Sängler, Uta Dahmen, and Olaf Dirsch. One size fits all: evaluation of the transferability of a new “learning” histologic image analysis application. *Applied Immunohistochemistry & Molecular Morphology*, 24(1):1–10, 2016.
- [21] Wouter Bulten, Kimmo Kartasalo, Po-Hsuan Cameron Chen, Peter Ström, Hans Pinckaers, Kunal Nagpal, Yuannan Cai, David F Steiner, Hester Van Boven, Robert Vink, et al. Artificial intelligence for diagnosis and gleason grading of prostate cancer: the panda challenge. *Nature medicine*, 28(1):154–163, 2022.
- [22] Gabriele Campanella, Shengjia Chen, Manbir Singh, Ruchika Verma, Silke Muehlstedt, Jennifer Zeng, Aryeh Stock, Matt Croken, Brandon Veremis, Abdulkadir Elmas, et al. A clinical benchmark of public self-supervised pathology foundation models. *Nature Communications*, 16(1):3640, 2025.
- [23] Xiyue Wang, Sen Yang, Jun Zhang, Minghui Wang, Jing Zhang, Wei Yang, Junzhou Huang, and Xiao Han. Transformer-based unsupervised contrastive learning for histopathological image classification. *Medical image analysis*, 81:102559, 2022.
- [24] Richard J Chen, Tong Ding, Ming Y Lu, Drew FK Williamson, Guillaume Jaume, Andrew H Song, Bowen Chen, Andrew Zhang, Daniel Shao, Muhammad Shaban, et al. Towards a general-purpose foundation model for computational pathology. *Nature Medicine*, 30(3):850–862, 2024.

8 Appendix

Table 2: Overview of different tasks created from the TCGA and PLCO cohorts.

Cohort	Target	Num WSIs	Organ	Origin
Organ Subtype	Subtype	22225	Various	TCGA
SKCM	Overall Survival	844	Skin	TCGA
PLCO	Overall Survival	2380	Prostate	PLCO
LGG/GBM	Subtype	3529	Brain	TCGA
KICH/KIRP/KIRC	Subtype	3207	Kidney	TCGA
PRAD	Overall Survival	525	Prostate	TCGA
	Subtype	525	Prostate	TCGA
BRCA	Overall Survival	1023	Breast	TCGA
	Subtype	1023	Breast	TCGA
	TP53 Mutation Prediction	1023	Breast	TCGA
	SPAT1 Mutation Prediction	1023	Breast	TCGA
	CDH1 Mutation Prediction	1023	Breast	TCGA
LUAD/LUSC	Subtype	1053	Lung	TCGA
	LUSC TP53 Mutation Prediction	408	Lung	TCGA
COAD/READ	Overall Survival	1318	Colon	TCGA
	TP53 Mutation Prediction	1318	Colon	TCGA
	KRAS Mutation Prediction	1318	Colon	TCGA
	Subtype	1903	Colorectal	TCGA

Listing 1: CPTAC-Query

```

SELECT
  collection_id as collection_id ,
  index.PatientID as patient_id ,
  index.StudyInstanceUID as study_id ,
  index as index ,
  sm_index as sm_index ,
  sm_instance_index as sm_instance_index ,
  sm_instance_index.SOPInstanceUID as slide_id ,
  sm_instance_index.SeriesInstanceUID as series_id ,
  sm_instance_index.PixelSpacing_0 as pixel_spacing ,
  CONCAT(
    TRIM(index.series_aws_url , '*') ,
    sm_instance_index.crdc_instance_uuid ,
    '.dcm'
  ) as url ,
  sm_index.primaryAnatomicStructureModifier_CodeMeaning as tissue
FROM
  (sm_instance_index
  LEFT JOIN index
    ON sm_instance_index.SeriesInstanceUID = index.SeriesInstanceUID)
  LEFT JOIN sm_index
    ON sm_instance_index.SeriesInstanceUID = sm_index.SeriesInstanceUID
WHERE
  index.Modality = 'SM'
  AND index.collection_id LIKE 'cptac_%'
  AND sm_instance_index.ImageType[3] = 'VOLUME'
  AND sm_index.illuminationType_code_designator_value_str = 'DCM:111744'

```

Listing 2: TCGA-Query

```

SELECT
  collection_id as collection_id ,
  index.PatientID as patient_id ,
  index.StudyInstanceUID as study_id ,

```

```

index as index,
sm_index as sm_index,
sm_instance_index as sm_instance_index,
sm_instance_index.SOPInstanceUID as slide_id,
sm_instance_index.SeriesInstanceUID as series_id,
sm_instance_index.PixelSpacing_0 as pixel_spacing,
CONCAT(
    TRIM(index.series_aws_url, '*'),
    sm_instance_index.crdc_instance_uuid,
    '.dcm'
) as url,
sm_index.primaryAnatomicStructureModifier_CodeMeaning as tissue
FROM
(sm_instance_index
LEFT JOIN index
    ON sm_instance_index.SeriesInstanceUID = index.SeriesInstanceUID)
LEFT JOIN sm_index
    ON sm_instance_index.SeriesInstanceUID = sm_index.SeriesInstanceUID
WHERE
index.Modality = 'SM'
AND index.collection_id LIKE 'tcga_%'
AND sm_instance_index.ImageType[3] = 'VOLUME'
AND sm_index.illuminationType_code_designator_value_str = 'DCM:111744'

```